

A Highly Selective Colorimetric Naked-Eye Probe for Hypochlorite Detection in Water

YU Qing¹, CHEN Xiao-li², ZHANG Qi-long^{1,3*}, LIU Hua³, YANG Xian-jiong³,
XU Hong³, HUANG Ya-li^{3*}, FENG Xing^{4*}, REDSHAW Carl⁵

1. School of Public Health, the Key Laboratory of Environmental Pollution Monitoring and Disease Control, Ministry of Education, Guizhou Medical University, Guiyang 550004, China
2. School of Clinical Medicine, Guizhou Medical University, Guiyang 550004, China
3. School of Basic Medical Science, Guizhou Medical University, Guiyang 550004, China
4. Guangdong Provincial Key Laboratory of Functional Soft Condensed Matter, School of Material and Energy, Guangdong University of Technology, Guangzhou 510006, China
5. Department of Chemistry & Biochemistry, University of Hull, Cottingham Road, Hull, Yorkshire HU6 7RX, UK

Abstract The real-time detection and monitoring of hypochlorites (ClO^-) in water is highly challenging. An excellent colorimetric “naked-eye” probe photoacid (PAH) was synthesized. PAH was confirmed using High-Resolution Mass Spectrometry (HRMS), ^1H NMR and ^{13}C NMR. The interaction between PAH and ClO^- was investigated via UV-Vis absorption spectrophotometry under different pH conditions. The results indicated that PAH was completely soluble in water, PAH displayed a yellow solution in a phosphate buffer with a pH of 2.0 to 5.0, and the maximum absorption peak was at 424 nm. PAH displayed a purple solution in a phosphate buffer with a pH of 6.0~12.0, and the maximum absorption peak was at 532 nm. After adding ClO^- to different pH systems, PAH discoloration and the UV-Vis absorption peak disappeared. The probe PAH exhibited specific selectivity and sensitivity for ClO^- detection with a low detection limit in the pH 5.0 phosphate buffer. After PAH reacted with ClO^- , the absorption peak of the probe at 424 nm gradually decreased, and a new absorption peak appeared at 532 nm. The probe displayed a vivid color-tunable process from yellow to purple then to colorless with a fast response time for ClO^- detection. However, other common 33 substances such as metal ions (Li^+ , Co^{2+} , Cr^{3+} , K^+ , Cd^{2+} , Pb^{2+} , Ca^{2+} , Hg^{2+} , Ba^{2+} , Cu^{2+} , Mg^{2+} , Ni^{2+} , Zn^{2+} , Al^{3+} and Fe^{3+}), anions (NO_2^- , I^- , AcO^- , ClO_4^- , SO_4^{2-} , CN^- , Br^- , CO_3^{2-} and F^-), reactive oxygen species ($\text{ROO}\cdot$, $\cdot\text{OH}$, H_2O_2 , $\cdot\text{O}_2^-$, $\cdot\text{BuOOH}$, $\cdot\text{BuO}$ and $^1\text{O}_2$) and reactive nitrogen species (ONOO^- and $\text{NO}\cdot$), did not cause changes in the color of the probe solution and the UV-Vis absorption spectrum. The above species had only a limited effect on detecting the ClO^- anion. When they coexisted with ClO^- , the probe also showed a similar solution color change, and the absorption peak at 424 nm disappeared. Meanwhile, the probe PAH could quantitatively detect the content of ClO^- with a detection limit of $5.39 \mu\text{mol} \cdot \text{L}^{-1}$ ($y = 1.58678 - 0.52451x$, $R^2 = 0.99852$). Furthermore, ClO^- concentration in the water system (84 disinfectant and tap water) was analyzed. The average concentration of ClO^- ion in the tap water measured by three parallel tests was $7.96 \mu\text{mol} \cdot \text{L}^{-1}$ with high recoveries rate. It showed that PAH could also be utilized to detect ClO^- quantitatively in real water systems.

Received: 2020-07-06; **accepted:** 2020-11-09

Foundation item: the National Natural Science Foundation of China (22065009, 22066007), the Science and Technology Foundation of Guizhou Province ([2019]2792), [2018]5779-14)

Biography: YU Qing, (1992—), postgraduate in School of Public Health, the Key Laboratory of Environmental Pollution Monitoring and Disease Control, Ministry of Education, Guizhou Medical University e-mail: 1432507000@qq.com

CHEN Xiao-li, (1996—), graduate in School of Clinical Medicine, Guizhou Medical University e-mail: 2422691291@qq.com

* Corresponding authors e-mail: gzuqlzhang@126.com; ylh6401@gmc.edu.cn; hyxhn@sina.com

The pH values were determined with a model pHs-25 pH meter. High-resolution mass spectrometry (HRMS) were performed in a micro TOF-Q II mass spectrometer (USA). $^1\text{H}/^{13}\text{C}$ NMR (400 MHz) spectra was recorded on a Bruker Advance 400 spectrometer(Germany), with DMSO- d_6 used as a solvent and tetramethylsilane (TMS) as an internal standard.

1.2 Experimental method

1.2.1 Synthesis of probe PAH

Probe PAH was synthesized according to the reported procedures^[12]. A mixture of 2, 3, 3-trimethylindolenine 1 (1.65 g, 0.01 mmol) and 1,2-oxathiolane 2,2-dioxide (1.26 g, 0.01 mmol) in toluene and stirred at 90 °C for 4 h under N_2 . The purple solid was collected by filtration, washed with cold ethylether, and dried in vacuo to afford 2,3,3-trimethyl-1-(3-sulfonatepropyl)-3H-indolium 2 (2.61 g, 89% yield). Without further purification, the synthesized compound 2 (100 mg, 0.36 mmol) and 2-hydroxybenzaldehyde (48 mg, 0.39 mmol) were added into anhydrous ethanol (2 mL). The mixture was allowed to reflux overnight. The orange solid was obtained by filtration (110 mg, 80% yield); ^1H NMR (400 MHz, d_6 -DMSO): δ 8.6~8.48 (m, 1H), 8.24 (*d*, J = 7.9 Hz, 1H), 7.99 (*d*, J = 8.2 Hz, 1H), 7.90~7.78 (m, 2H), 7.65~7.53 (m, 2H), 7.44 (*t*, J = 7.7 Hz, 1H), 7.04~6.89 (m, 2H), 4.90~4.66 (m, 2H), 2.62 (*t*, J = 6.4 Hz, 2H), 2.22~2.05 (m, 2H), 1.84~1.62 (m, 6H); ^{13}C NMR (100 MHz, d_6 -DMSO) δ 182.27 (s), 159.55 (s), 149.19 (s), 144.01 (s), 141.45 (s), 136.28 (s), 130.28 (s), 129.66 (s), 123.52 (s), 121.86 (s), 120.59 (s), 117.15 (s), 115.61 (s), 111.97 (s), 52.43 (s), 47.87 (s), 46.06 (s), 26.97 (s), 25.12 (s). HRMS: m/z $[\text{M} + \text{Na}]^+$ = 408.126; Calcd: 407.120. The $^1\text{H}/^{13}\text{C}$ NMR data is consisting with the previously reported data^[12].

1.2.2 Preparation of solutions

Phosphate buffer saline (PBS) with different pH from 2.0 to 12.0 was prepared from disodium hydrogen phosphate, dihydrogen phosphate and sodium chloride in a certain proportion with ultrapure water^[13]. The 0.5 mmol \cdot L⁻¹ stock solution of probe PAH was prepared in an aqueous solution of PBS (0.01 mol \cdot L⁻¹, pH 5.0). The 0.01 mol \cdot L⁻¹ stock solutions of the metal ions and various anions were dissolved in an aqueous solution of PBS (0.01 mol \cdot L⁻¹, pH 5.0). The 0.01 mol \cdot L⁻¹ stock solutions of reduced vitamin C (Vc) and glutathione (GSH) were prepared directly from the solids in aqueous solution of PBS (0.01 mol \cdot L⁻¹, pH 5.0). Hypochlorites were derived from sodium hypochlorite. The stock solution of ClO^- was prepared with 0.01 mol \cdot L⁻¹ sodium hydroxide solution and standardized at 292 nm using an extinction coefficient 350 M⁻¹ \cdot cm⁻¹ at pH 12.0^[14], then

diluting the stock solution of ClO^- to 8 mmol \cdot L⁻¹. The 0.01 mol \cdot L⁻¹ stock solution of other reactive oxygen species (ROS) and reactive nitrogen species (RNS) were prepared according to the literature^[15].

1.2.3 General procedure for analysis

Before conducting the spectroscopic measurements, the corresponding solutions of probe PAH and the reactive species (metal ions, anions, ROS and RNS) were freshly prepared. For UV-Vis selective experiments, test solutions were prepared by placing 0.6 mL of the probe PAH solution (0.5 mmol \cdot L⁻¹) and 0.12 mL of reactive species solutions in the absence and presence of 0.12 mL of ClO^- solutions (8 mmol \cdot L⁻¹) into a 3 mL cuvette, and then diluting the solution to 3 mL with PBS (0.01 mol \cdot L⁻¹, pH 5.0). For UV-Vis titrations, 0.6 mL of the probe PAH solution and different amounts of ClO^- was added into a 3 mL cuvette. These solutions were diluted with PBS (0.01 mol \cdot L⁻¹, pH 5.0) to 3 mL and mixed, then the spectra of these solutions were immediately recorded through the UV-Vis method.

2 Results and discussion

2.1 The pH effect to PAH

Previous reports indicated that PAH would undergo decomposition depending on the pH of the aqueous solution^[16]. Thus, the pH-dependent stability of PAH was investigated in different buffered solutions from pH 2.0 to 12.0. As shown in Fig.1, the probe in pH 2 solution exhibited a yellow color and a well-resolved absorption band range from 300~500 nm with a maximum absorption peak at 424 nm, as the pH increased from 2.0 to 5.0, the absorption peak at 424 nm gradually decreased, which may be due to protonation of the terminal SO_3^- group. On continuing to increase the pH from 6.0 to 12.0, the yellow absorption intensity was decreased with a new absorption peak appearing at 532 nm, which may be due to the phenol group ($-\text{OH}$) undergoing a neutralization reaction leading to a sizeable red-shifted absorption peak^[16]. Subsequently, the more extended wavelength absorption peak shows a gradual decrease with a tunable color from yellow to purple then to pink, indicating that the probe would be slowly hydrolysis when the $\text{pH} \geq 9.0$ ^[16]. These results are consistent with reported observations^[16]. On the other hand, It is noted that the response time of PAH toward ClO^- detection at $\text{pH} < 7.0$ is faster than at $\text{pH} > 7.0$, which may be attributed to the more muscular oxidation activity of hypochlorite in acidic conditions. Thus, considering the stability of probe PAH and the practical application environment, all detect experiments were performed in pH 5.0 buffered solution.

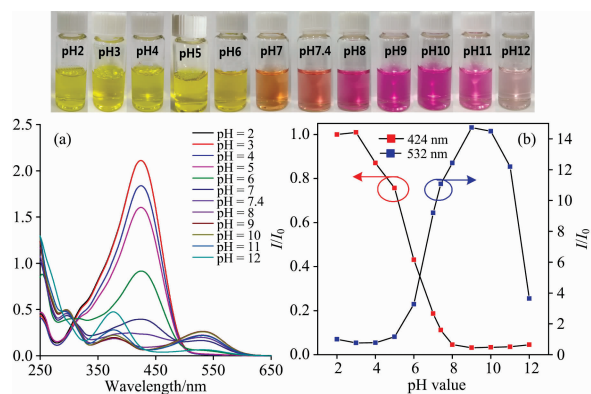


Fig. 1 The change of UV-Vis spectra (a) and line graph (b) of probe PAH ($0.1 \text{ mmol} \cdot \text{L}^{-1}$) in the range from pH 2.0 ~ 12.0 using PBS as buffer solution; The color change of photography of probe PAH with the pH value increases under natural light (inset)

2.2 Selectivity recognition toward ClO^-

A colorimetric probe's high selectivity and sensitivity are key parameters for real applications in tap water monitoring and in vivo studies. Thus, the UV-Vis response of PAH toward metal ions and anions, reactive oxygen species (ROS) and reactive nitrogen species (RNS) was evaluated in pH 5.0

buffered solution as presented in Fig.2 and in Fig.S3. Clearly, except for ClO^- , the PAH solution ($0.1 \text{ mmol} \cdot \text{L}^{-1}$) still displays a yellow color, and the corresponding UV-Vis spectra indicated that the absorption behavior exhibited slight changes after the addition of 4 equiv. The various extra species, such as metal ions and anions, reactive oxygen species (ROS) and reactive nitrogen species (RNS). Furthermore, by adding the same concentration of ClO^- into the solution containing the PAH and the metal ion species, the absorption peak at 424 nm disappeared and the solution color changed from yellow to colorless [Figure 2 (a) and (d)]. The results indicated that the PAH exhibited a highly selective response toward ClO^- with great anti-interference ability to other species. Furthermore, when the ClO^- adding into the mixture of PHA and various anions, the UV-Vis spectra show only slight changes excepted the reductive anions, such as I^- , ONOO^- , NO_2^- , GSH and Vc anion. [Figure 2 (b), (c), (e) and (f)] For example, in the presence of I^- anions, the solution color changes from yellow to purple, which may be attributed to the strong oxidation activity of ClO^- , which can preferentially react with the I^- or ONOO^- , NO_2^- , GSH and Vc and consume ClO^- via a redox reaction process.

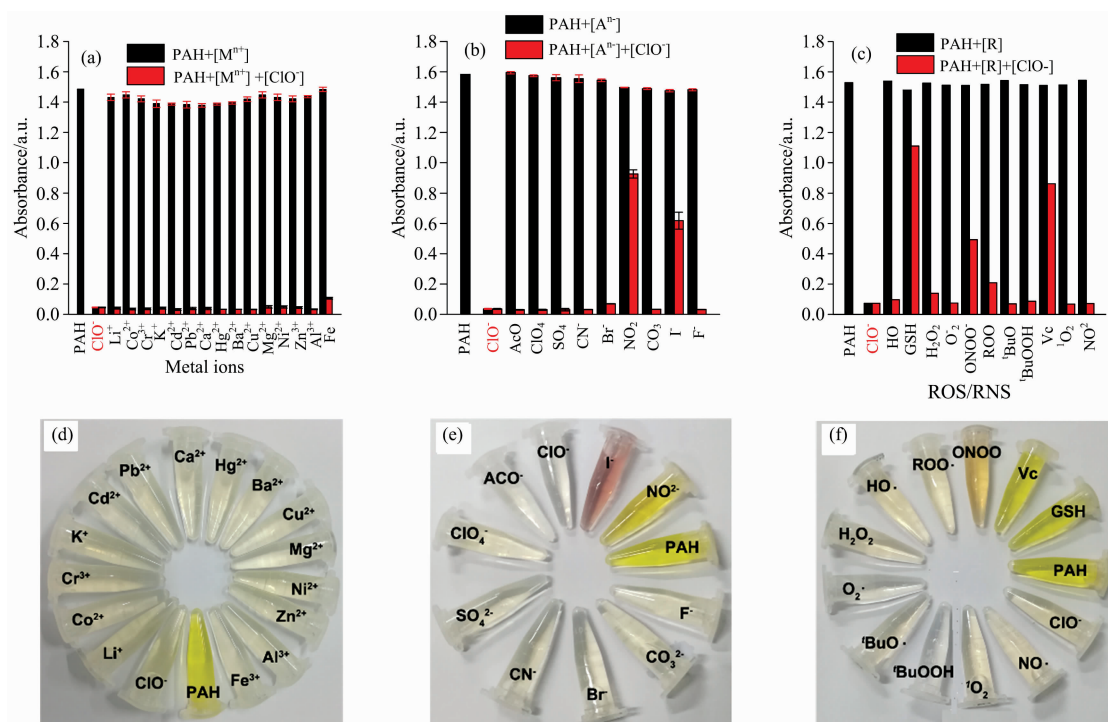


Fig. 2 Absorption intensity (a—c) at 424 nm of probe PAH ($0.1 \text{ mmol} \cdot \text{L}^{-1}$) with addition of different species ($0.4 \text{ mmol} \cdot \text{L}^{-1}$) in the absence/presence of ClO^- ($0.4 \text{ mmol} \cdot \text{L}^{-1}$) in PBS solution ($0.01 \text{ mol} \cdot \text{L}^{-1}$, pH 5.0), Error bar=RSD ($n=3$); Visible color (d—f) of probe PAH toward ClO^- ($0.4 \text{ mmol} \cdot \text{L}^{-1}$) in different species under sunlight

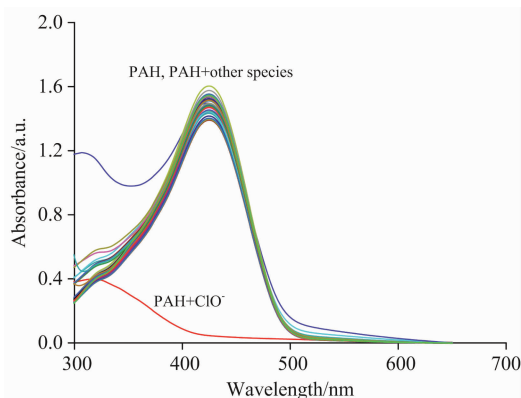


Fig. S3 UV-Vis spectra of PAH ($0.1 \text{ mmol} \cdot \text{L}^{-1}$) with addition of nitrate salts of Li^+ , Co^{2+} , Cr^{3+} , K^+ , Cd^{2+} , Pb^{2+} , Ca^{2+} , Hg^{2+} , Ba^{2+} , Cu^{2+} , Mg^{2+} , Ni^{2+} , Zn^{2+} , Al^{3+} and Fe^{3+} ($0.4 \text{ mmol} \cdot \text{L}^{-1}$), sodium salts of NO_2^- , I^- , AcO^- , ClO_4^- , SO_4^{2-} , CN^- , Br^- , CO_3^{2-} and F^- ($0.4 \text{ mmol} \cdot \text{L}^{-1}$), ClO^- ($0.4 \text{ mmol} \cdot \text{L}^{-1}$), GSH, Vc and ROS/RNS of ONOO^- , $\text{ROO} \cdot$, $\cdot\text{OH}$, H_2O_2 , $\cdot\text{O}_2^-$, $^1\text{BuOOH}$, $^1\text{BuO} \cdot$, $^1\text{O}_2$ and $\text{NO} \cdot$ ($0.4 \text{ mmol} \cdot \text{L}^{-1}$) in PBS solution ($0.01 \text{ mol} \cdot \text{L}^{-1}$, pH 5)

Further, the effect of I^- , ONOO^- , NO_2^- , GSH and Vc toward ClO^- detection was investigated. Take the iodide ion (I^-) as an example (Fig. 3). The mixture of PAH and I^- displays a yellow color, and a maximum absorption peak at 424 nm. While adding the ClO^- to the solution, the UV-Vis spectra indicated a new absorption peak at 550 nm, and upon increasing the concentration from 0 to $1.6 \text{ mmol} \cdot \text{L}^{-1}$, the new absorption peak at 550 nm disappeared. The chemical reaction involved the following two steps, (1) the presence of I^- can react with ClO^- to achieve I_2 , (2) both the presence of the oxidant of I_2 and the extra ClO^- would further decompose the probe^[17]. Thus, the successive chemical reaction process would lead to the solution colour change from yellow to purple and then to colorless, and the whole process could be identified by the naked-eye. Similar absorption behavior was observed in the presence of ONOO^- , NO_2^- , GSH and Vc systems and the UV-Vis spectra are illustrated in Fig. S4.

2.3 UV-Vis absorbance response of probe PAH towards ClO^-

The recognition ability of probe PAH toward ClO^- was measured using UV-Vis titrations in buffered aqueous solution (PBS, $0.01 \text{ mol} \cdot \text{L}^{-1}$, pH 5.0). As shown in Fig. 4, with increasing ClO^- concentrations, the absorption peak of probe PAH at 424 nm gradually decreased and the short absorption wavelength centering around 296 nm gradually increased, accompanied by a change in the color of the solution from yellow to colorless. Moreover, a well-defined isosbestic point was observed at 315 nm, indicating the formation of a single

new species. In addition, the UV-Vis titration experiments between the corresponding absorbance values at 424 nm and ClO^- concentrations exhibited an excellent linear correlation with a high coefficient ($y = 1.58678 - 0.52451x$, $R^2 = 0.99852$) in the range of $0 \sim 0.28 \text{ mmol} \cdot \text{L}^{-1}$ [Fig. 4(c)]. Thus, the detection limit of probe PAH for ClO^- detection was determined to be $5.39 \mu\text{mol} \cdot \text{L}^{-1}$ according to the IUPAC definition ($\text{CDL} = 3S_b/m$, S_b is the standard deviation of the blank samples, m is the slope of the linear equation) from 10 blank solutions^[18]. These results illustrated that probe PAH has the excellent capability for the qualitative and quantitative determination of ClO^- with high sensitivity in total aqueous solutions.

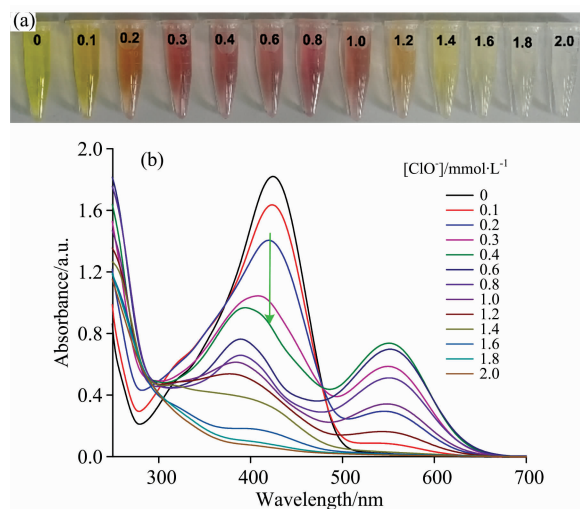


Fig. 3 UV-Vis absorption spectra (b) of PAH ($0.1 \text{ mmol} \cdot \text{L}^{-1}$) in the presence of I^- toward various concentration of ClO^- in PBS buffer solution ($0.01 \text{ mol} \cdot \text{L}^{-1}$, pH 5.0); The change of visible color (a) of probe PAH toward ClO^- under sunlight

It is noteworthy that on the addition of a small amount of ClO^- to the solution of probe PAH, a new absorption band appeared in the range from $500 \sim 570 \text{ nm}$, while following an increase in the concentration of ClO^- , the absorption gradually disappeared again. We hypothesized that the new long absorption band originated from the degraded compound of indolinium, which strongly agrees with our experiment results (Fig. S5).

2.4 The pH effect toward ClO^- detection

The pH value of the environment is a crucial parameter that can affect the selectivity, sensitivity, and detection limit of a probe^[19]. Carefully, the absorption behavior of probe PAH toward ClO^- was investigated over the relevant pH range from 2.0 to 12.0, respectively (Fig. 5 and Fig. S6). The maximum absorption peak of probe PAH is at 424 nm within a pH range of $2.0 \sim 5.0$ with a yellow color solution, but when treated with ClO^- , the solution color dramatically changed

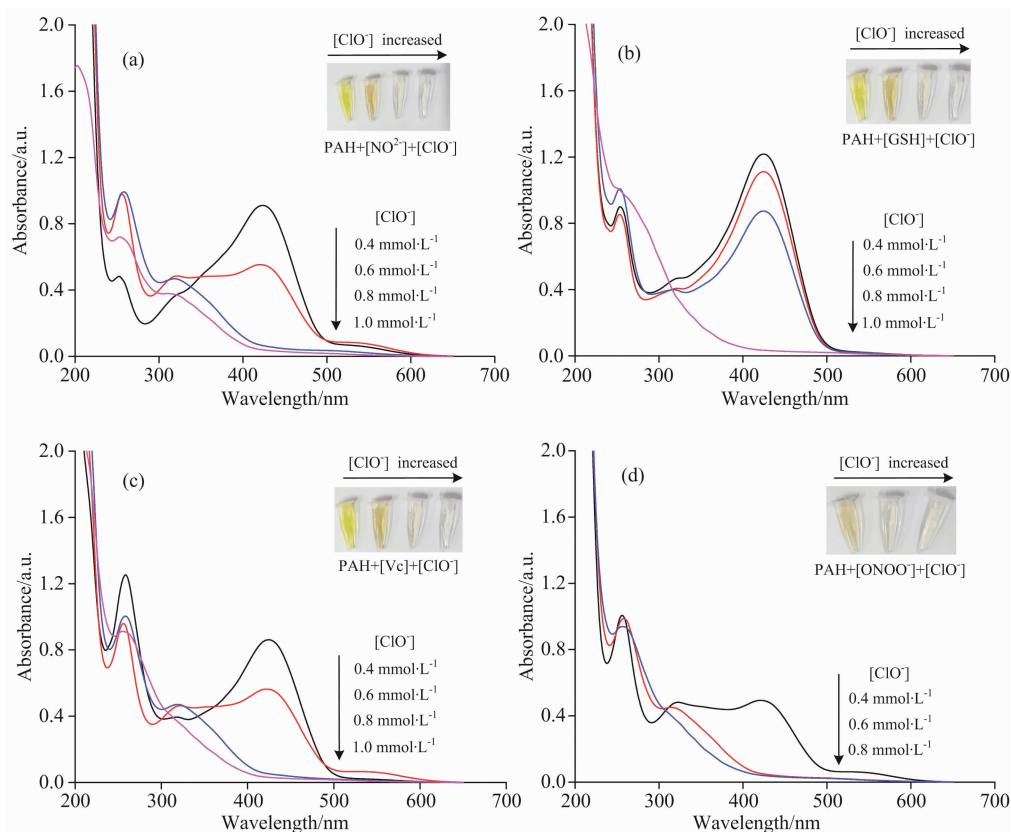


Fig. S4 UV-Vis absorption spectra (a—d) of PAH ($0.1 \text{ mmol} \cdot \text{L}^{-1}$) with the addition of NO_2^- , GSH, Vc, ONOO^- toward various concentration of ClO^- in PBS buffer solution ($0.01 \text{ mol} \cdot \text{L}^{-1}$, pH 5.0); The change of visible color of probe PAH toward ClO^- under sunlight (inset)

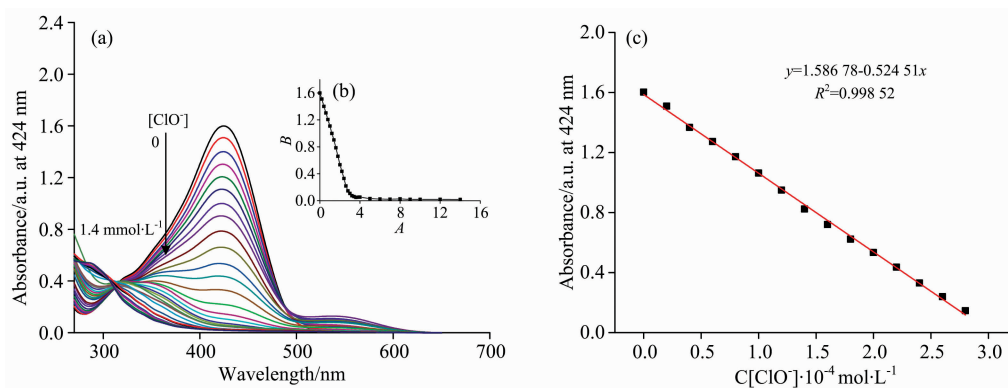


Fig. 4 UV-Vis spectra (a) of probe PAH ($0.1 \text{ mmol} \cdot \text{L}^{-1}$), changing of the absorption intensity (b) at 424 nm of probe PAH upon addition of increasing concentrations ($0 \sim 1.4 \text{ mmol} \cdot \text{L}^{-1}$) of ClO^- in PBS ($0.01 \text{ mol} \cdot \text{L}^{-1}$, pH 5.0) and linearity of absorption intensity (c) of probe PAH with the addition of ClO^- from $0 \sim 0.28 \text{ mmol} \cdot \text{L}^{-1}$. Error bar = RSD ($n=3$)

from yellow to colorless, and the maximum absorption peak of 424 nm disappeared. On the other hand, the neutralized PAH at $\text{pH} > 6.0$, displayed two absorption peaks at 424 and 550 nm, respectively. However, when treated with ClO^- from 0 to $1.4 \text{ mmol} \cdot \text{L}^{-1}$, both absorption peaks gradually decreased, and even disappeared, and the solution containing PAH turned from purple to colorless. These results indicated

that the PAH is a highly sensitive, “naked-eye” colorimetric sensor for ClO^- detection in aquatic environments. More importantly, the presence of metal ions and anions, ROS and RNS only provide a limited ClO^- detection disruption. Thus the excellent probe PAH can be applied for detecting the ClO^- in natural water samples with significantly more complex compositions.

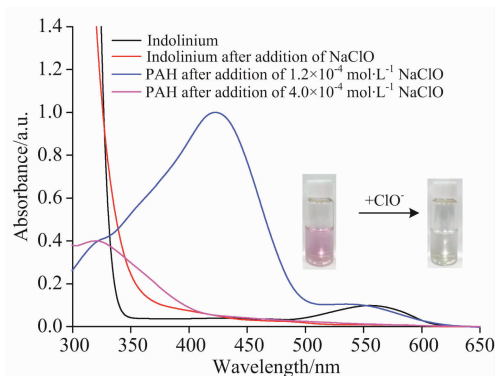


Fig. S5 UV-Vis absorption spectra of indolinium in the absence/presence of ClO^- in aqueous solution and UV-Vis absorption spectra of probe PAH ($0.1 \text{ mmol} \cdot \text{L}^{-1}$) in the presence of ClO^- ($0.12 \text{ mmol} \cdot \text{L}^{-1}$ or $0.4 \text{ mmol} \cdot \text{L}^{-1}$) in PBS ($0.01 \text{ mol} \cdot \text{L}^{-1}$, pH 5.0); Photography of indolinium in the absence/presence of ClO^- (inset)

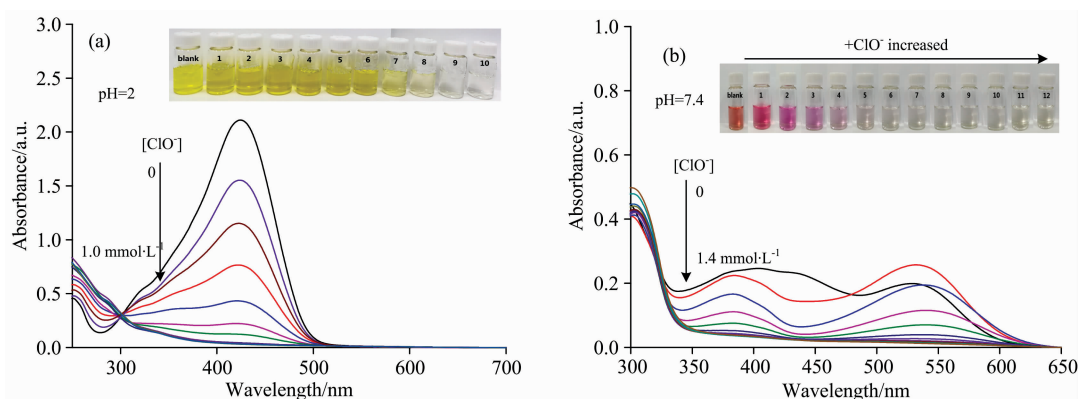
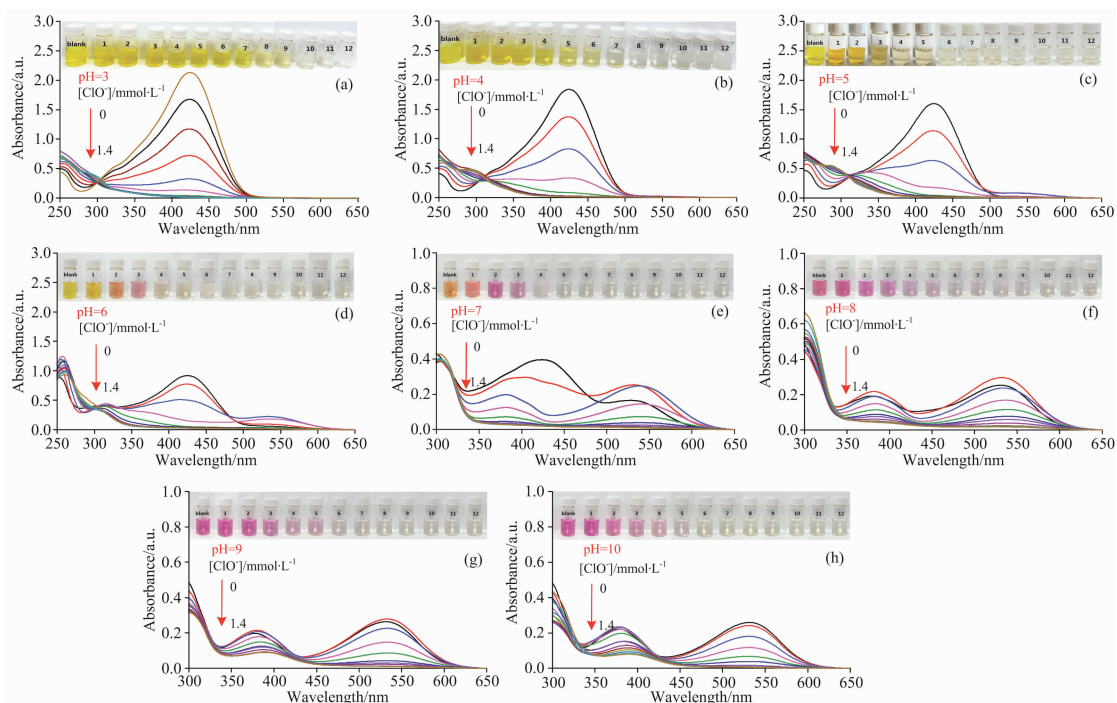


Fig. 5 UV-Vis spectra of probe PAH ($0.1 \text{ mmol} \cdot \text{L}^{-1}$) with the addition of ClO^- ($0 \sim 1.4 \text{ mmol} \cdot \text{L}^{-1}$) in PBS ($0.01 \text{ mol} \cdot \text{L}^{-1}$) in pH 2.0 (a), pH 7.4 (b), respectively; The photography change of visible color of probe PAH toward ClO^- under sunlight (inset)



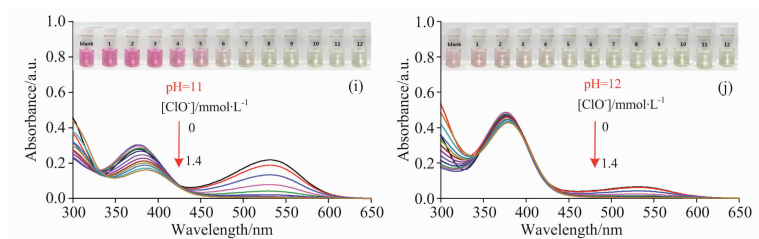


Fig. S6 UV-Vis spectra of probe PAH ($0.1 \text{ mmol} \cdot \text{L}^{-1}$) with the addition of ClO^- ($0 \sim 1.4 \text{ mmol} \cdot \text{L}^{-1}$) in PBS ($0.01 \text{ mol} \cdot \text{L}^{-1}$) in pH 3.0 (a), pH 4.0 (b), pH 5.0 (c), pH 6.0 (d), pH 7.0 (e), pH 8.0 (f), pH 9.0 (g), pH 10.0 (h), pH 11.0 (i), pH 12.0 (j), respectively; The photography change of visible color of probe PAH toward ClO^- under sunlight (inset)

2.5 Recognition mechanism

The pH-dependence of the UV-Vis spectra showed that the probe PAH exhibited color-tunable properties from yellow to purple then to pink. There were two pathways to the hydrolysis of PAH in acidic and alkaline environment. In acidic environments (pH 2.0~5.0), the H^+ would attack the SO_3^- to balance the electric charge form $[\text{PAH}]^+$, and the PAH solution keep yellow color; while under alkaline conditions, the neutralization reaction preferred to occur with $[\text{PAH}]^-$ between the OH group with an extra OH^- in the molecular structure of PAH; hydrolysis of PAH under strongly alkaline conditions, and the solution changed to purple colour, due to the intramolecular interaction. On the other hand, the oxidative property of the hypochlorite anion could improve under acidic conditions and can accelerate the oxidation reaction compared to under alkaline conditions (Fig. S7). Based on our experiment results, a possible recognition mechanism was proposed in Scheme 2.

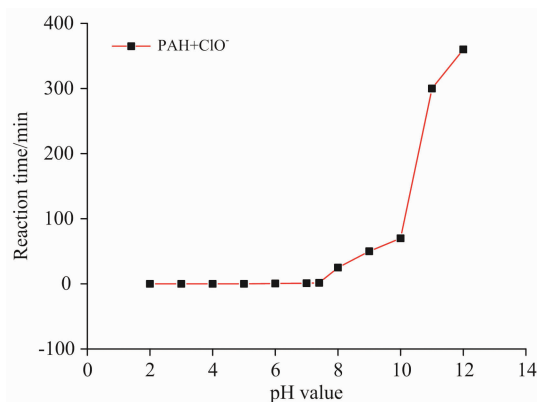
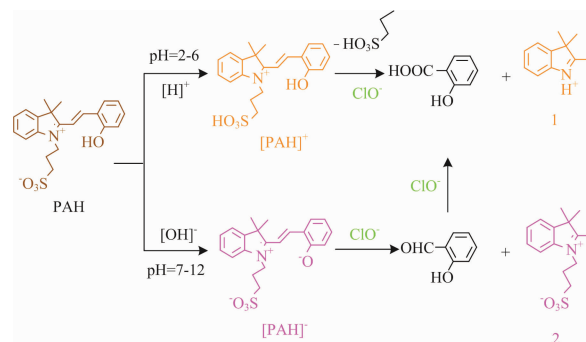


Fig. S7 Comparison of the interaction time between PAH ($0.1 \text{ mmol} \cdot \text{L}^{-1}$) and ClO^- ($0.8 \text{ mmol} \cdot \text{L}^{-1}$) in aqueous solution of PBS ($0.01 \text{ mol} \cdot \text{L}^{-1}$, pH 2.0~12.0)

Firstly, in the presence of ClO^- , oxidation cleavage of the $\text{C}=\text{C}$ double of PAH would afford the 2-hydroxybenzoic acid/salicylaldehyde and indolinium derivative depending on the pH conditions. In the pH range from 7.0 to 12.0, when the $[\text{PAH}]^-$ encountered ClO^- , it would be

oxidized to 2 and salicylaldehyde, while at pH 2.0~6.0, the $[\text{PAH}]^+$ can be oxidized to indolinium fragment 1 with 2-hydroxybenzoic acid. The detailed information of the molecular structures was supported by mass spectrometry and is listed in Fig. S8—Fig. S10.



Scheme 2 The proposed recognition mechanism of probe PAH toward ClO^-

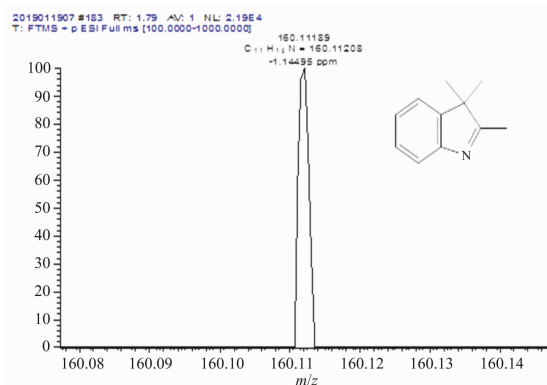


Fig. S8 HRMS of intermediate 1

The peak (m/z) at 160.111 89 corresponds to $[\text{M}+\text{H}]^+$ ion (Calcd.: 159.10)

On titration of hypochlorite under acidic conditions, HRMS data manifested the peaks at $m/z=160.111 89$ and $139.038 97$, corresponding to the intermediates 1 and 2-hydroxybenzoic acid; while under basic conditions, HRMS gives result for $m/z=123.044 06$ and $282.115 84$ consistent with intermediate 2 and salicylaldehyde, respectively.

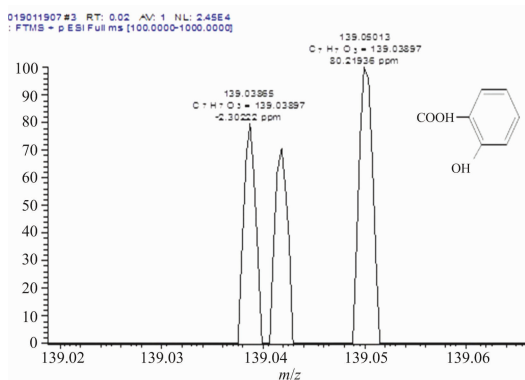


Fig. S9 HRMS of 2-hydroxybenzoic acid

The peak (m/z) at 139.038 97 corresponds to $[M+H]^+$ ion (Calcd: 138.03)

2.6 Detection of ClO^- in 84 disinfectant and tap water samples

Hypochlorite is widely used in our daily life. Thus, the probe PAH had been applied to analyse the content of ClO^- in real samples (such as 84 disinfectant and tap water). The real sample was filtered for the removal of insoluble species. In a PBS ($0.01 \text{ mol} \cdot \text{L}^{-1}$, pH 5.0) solution of 3 mL containing the probe PAH ($0.1 \text{ mmol} \cdot \text{L}^{-1}$), the sample of 84 disinfectants was added with different volumes of 2.0, 4.0, 6.0 μL , respectively. The calculated concentration of ClO^-

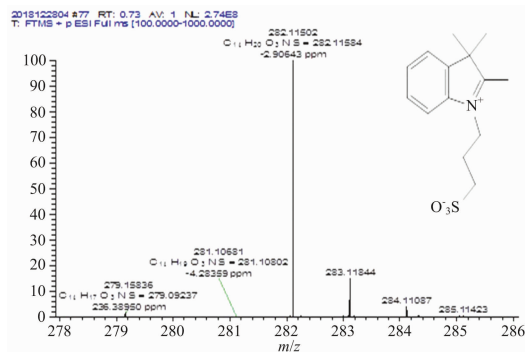


Fig. S10 HRMS of intermediate 2

The peak (m/z) at 282.115 84 corresponds to $[M+H]^+$ ion (Calcd: 281.11)

of this 84 disinfectant sample is (151 ± 6.68) $\text{mmol} \cdot \text{L}^{-1}$ (Table 1), According to the linear regression equation of UV-Vis titration ($y = 1.58678 - 0.52451x$, $R^2 = 0.99852$). Further, the content of ClO^- in tap water and purified water were also measured under the same conditions, and the calculated concentration of ClO^- is $7.96 \mu\text{mol} \cdot \text{L}^{-1}$ for the tap water sample (Table 1). Except for one sample, the percentage recoveries were in the range of 93% ~ 103%. These results indicated that the probe PAH could potentially be used for the quantitative detection of ClO^- concentrations in real water samples.

Table 1 Determination of ClO^- concentrations in real samples

Sample name	Added ClO^- $/(\mu\text{mol} \cdot \text{L}^{-1})$	Found ClO^- $/(\mu\text{mol} \cdot \text{L}^{-1})^b$	Determined ClO^- $/(\mu\text{mol} \cdot \text{L}^{-1})$	Recovery /%
84 disinfectant	40.00 ^a	54.44 ± 1.36	151 ± 6.68	98.35
	60.00	77.24 ± 0.32		103.57
	80.00	96.98 ± 3.01		102.35
	0.00	7.96 ± 1.2		
Tap water	40.00	43.75 ± 1.76	7.96	89.48
	60.00	64.28 ± 2.47		93.87
	80.00	87.42 ± 2.86		99.33

Note: a: Mean ± standard deviation ($n=3$); b: diluted 10000-fold mother solution of 84-disinfectant

3 Conclusions

In conclusion, based on the oxidative activity of ClO^- , the PAH can be utilized as a highly selective colorimetric naked-eye probe for ClO^- detection via oxidative cleavage of itself in absolute aqueous solution, which leads to a tunable color process from yellow to purple then to colorless. The specificity of probe PAH can work in water environments,

and coexisting ions only show a slight effect on ClO^- detection. More importantly, acidic solid conditions accelerate the response time. Moreover, PAH exhibited a fast response time and naked eye detection toward ClO^- at various pH values with highly-sensitive detection at pH 5.0. We have also successfully applied the probe to detect ClO^- in real water samples. This research will open up new avenues for developing novel “naked-eye” probes for the detection of environmental pollutants in an absolute aqueous system.

References

- [1] Strzepa A, Pritchard K A, Dittel B N. *Cellular Immunology*, 2017, 317: 1.
- [2] MA Jie, DONG Fa-qin, HUO Ting-ting, et al. *Spectroscopy and Spectral Analysis*, 2018, 38(5): 1492.
- [3] Yue Y K, Huo F J, Yin C X, et al. *Analyst*, 2016, 141: 1859.
- [4] WANG Qing-ming, LEI Jin, WANG Wen-ling, et al. *Spectrochimica Acta Part A: Molecular and Biomolecular Spectroscopy*, 2019, 211: 239.
- [5] Lin P, Chai F, Zhang R, et al. *Microchimica Acta*, 2016, 183(3): 1235.
- [6] Claver J B, Mir6n M C V, Capit6n-Vallvey L F. *Analytica Chimica Acta*, 2004, 522(2): 267.
- [7] Gallina A, Pastore P, Magno F. *Analyst*, 1999, 124(10): 1439.
- [8] Ministry of Health of the People's Republic of China, Standardization Administration of the P. R. C. GB 5749—2006 Sanitary Standards for Drinking Water, 2006.
- [9] Han Q, Zhou F, Wang Y, et al. *Molecules*, 2019, 24(13): 2455.
- [10] Ning Y Y, Cui J H, Lu Y W, et al. *Sensors and Actuators B: Chemical*, 2018, 269: 322.
- [11] Feng X, Zhang J, Tang B Z, et al. *Journal of Materials Chemistry C*, 2019, 7: 6932.
- [12] Shi Z, Peng P, Liao Y, et al. *Journal of the American Chemical Society*, 2011, 133(37): 14699.
- [13] Jiang Y, Wu S, Jin C, et al. *Sensors and Actuators B: Chemical*, 2018, 265: 365.
- [14] Wang Z, Zhang Y, Song J, et al. *Dyes and Pigments*, 2019, 161: 172.
- [15] Wang Z, Zhang Y, Song J, et al. *Sensors and Actuators B: Chemical*, 2019, 284: 148.
- [16] Abeyrathna N, Liao Y. *Journal of Physical Organic Chemistry*, 2016, 196: 30(8): 1.
- [17] Wang C, Ji H, Li M, et al. *Faraday Discussions*, 2017, 427.
- [18] ZHOU Gao, FENG Feng, CHEN Ze-zhong, et al. *Spectroscopy and Spectral Analysis*, 2017, 37(9): 2799.
- [19] Feng X, Li Y, Tang B Z, et al. *Advanced Functional Materials*, 2018, 28(35): 1802833.

一种用于水中次氯酸根检测的高选择性裸眼比色探针

余 青¹, 陈晓丽², 张奇龙^{1,3*}, 刘 华³, 杨先炯³, 徐 红³,
黄亚励^{3*}, 冯 星^{4*}, REDSHAW Carl⁵

1. 贵州医科大学公共卫生学院教育部环境污染监测与控制重点实验室, 贵州 贵阳 550004
2. 贵州医科大学临床医学院, 贵州 贵阳 550004
3. 贵州医科大学基础医学院, 贵州 贵阳 550004
4. 广东工业大学材料与能源学院, 广东省功能性软冷凝物质重点实验室, 广东 广州 510006
5. Department of Chemistry & Biochemistry, University of Hull, Cottingham Road, Hull, Yorkshire HU6 7RX, UK

摘 要 实时检测和监测水中的次氯酸根离子(ClO^-)是极富挑战性的研究工作。报道了一种光学性能优异、“裸眼”可分辨的比色型探针分子(PAH)。首先利用高分辨质谱,核磁共振氢谱和核磁共振碳谱等方法对目标探针分子(PAH)的结构进行表征。随后,利用紫外-可见吸收光谱考察了不同 pH 缓冲溶液条件下探针 PAH 与次氯酸根离子的相互作用。结果显示,水溶性的探针分子 PAH 在 pH 值为 2.0~5.0 的磷酸盐缓冲液中为黄色溶液,其最大吸收峰在 424 nm 处;在 pH 值为 6.0~12.0 的磷酸盐缓冲液中 PAH 为紫色溶液,最大吸收峰在 532 nm 处;在不同 pH 缓冲液体系中分别加入次氯酸根离子,肉眼可观察 PAH 溶液颜色褪去,紫外-可见吸收光谱显示在 424 nm 处的特征吸收峰逐渐降低并在 532 nm 处出现新的吸收峰,溶液颜色从黄色到紫色然后到无色,特征峰明显消失。进一步优化了实验条件,发现在 pH 5.0 的磷酸盐缓冲液中,探针分子 PAH 对 ClO^- 离子具有特定的选择性和灵敏度,并且具有较低检出限等优点;在优化的条件下,探究了常见的金属离子、阴离子等共存条件下,对探针分子 PAH 检测次氯酸根离子的干扰影响。实验发现,常见的金属离子(Li^+ , Co^{2+} , Cr^{3+} , K^+ , Cd^{2+} , Pb^{2+} , Ca^{2+} , Hg^{2+} , Ba^{2+} , Cu^{2+} , Mg^{2+} , Ni^{2+} , Zn^{2+} , Al^{3+} 和 Fe^{3+}),阴离子(NO_2^- , I^- , AcO^- , ClO_4^- , SO_4^{2-} , CN^- , Br^- , CO_3^{2-} 和 F^-),活性氧($\text{ROO}\cdot$, $\cdot\text{OH}$, H_2O_2 , $\cdot\text{O}_2^-$, $^1\text{BuOOH}$, $^1\text{BuO}\cdot$ 和 $^1\text{O}_2$),和活性氮(ONOO^- 和 $\text{NO}\cdot$)等 33 种物质对探针分子检测 ClO^- 离子的干扰较小。同时,探针 PAH 可以定量检测次氯酸根离子($y=1.586\ 78-0.524\ 51x$, $R^2=$

0.998 52), 检出限为 $5.39 \mu\text{mol} \cdot \text{L}^{-1}$ 。此外, 对水体系(84 消毒剂和自来水)中的次氯酸根离子浓度进行分析, 三次平行试验测得自来水中次氯酸根离子的平均浓度为 $7.96 \mu\text{mol} \cdot \text{L}^{-1}$, 平均加标回收率高, 表明探针 PAH 还可用于定量检测实际水体系中的次氯酸根离子。

关键词 比色探针; 次氯酸根离子; 快速反应; 高选择性

(收稿日期: 2020-07-06, 修订日期: 2020-11-09)

* 通讯作者